

Resonance Auger spectra of free Rb atoms

H. Aksela, R. Lakanen, S. Aksela, and O.-P. Sairanen
Department of Physics, University of Oulu, SF-90570 Oulu, Finland

A. Yagishita

Photon Factory, National Laboratory for High Energy Physics, Oho-machi, Tsukuba-gun, Ibaraki 305, Japan

M. Meyer, Th. Prescher, E. von Raven, M. Richter, and B. Sonntag
II Institut für Experimentalphysik, Universität Hamburg, D-2000 Hamburg 50, West Germany
 (Received 4 April 1988)

Resonance Auger electron spectra of atomic Rb are studied both experimentally and theoretically. $3d_{5/2}$ electrons were excited selectively by the monochromated synchrotron radiation to $5p$ orbitals, and the spectrum of the ejected electrons was measured in the kinetic energy range of 7–95 eV. The experimental spectrum is compared with the calculated theoretical profile. For comparison the normal $3d$ Auger spectrum was also measured using electron-impact excitation.

INTRODUCTION

Resonance Auger spectra of rare gases Xe, Kr, and Ar have been studied recently by several authors.^{1–9} It has been found that besides the expected Auger-type transitions where the excited core electron remains as the spectator during the decay process also strong shake-up peaks appear in the spectra. Especially in the case of Ar $2p \rightarrow 3d$ excitation the lines due to $3d \rightarrow 4d$ shake up during the Auger decay were found to be very strong, in fact more intense than the Auger lines where the $3d$ electron remains as the spectator.⁹ Also, for Kr strong shake-up lines have been found especially when the $3d$ electrons were excited to higher np levels ($n = 6, 7, \text{ and } 8$).⁸ As the next neighbor to Kr resonance Auger spectra of Rb are of special interest in regard to these shake-up processes. Due to the extra $5s$ electron the spectra are expected to show also additional fine structure compared to corresponding spectra of closed-shell Kr atoms.

The normal Auger electron spectra of Rb have been studied by Menzel and Mehlhorn¹⁰ using electron-impact excitation. The *MNN* Auger spectrum was complicated by the overlapping broad $3p^5 \rightarrow 3d^9 4s^1 4p^6 5s^1$ and $3p^5 \rightarrow 3d^9 4s^2 4p^5 5s^1$ Coster-Kronig spectra. Furthermore, very strong satellite structure associated to $3d^9 \rightarrow 4s^1 4p^5 5s^1$ Auger transitions was found. The behavior of these satellite structures in the resonance Auger spectrum is therefore of special interest.

The $3d$ absorption spectrum of Rb has been measured and analyzed by Mansfield and Connerade.^{11–12} Based on the $Z + 1$ approximation Mårtensson and Johansson suggested an alternative interpretation for some absorption peaks.¹³ A better understanding of the experiment was later on achieved by applying configuration-mixing calculations.¹⁴

Ion-yield spectra of Rb have been measured by Koizumi *et al.*¹⁵ at Photon Factory. They show that Rb^{2+} ions form the main contribution and also Rb^{3+} has remarkable intensity but singly charged Rb ions do not show any

enhancement at $3d$ resonances. In order to map the multistep decay channels the knowledge of the energy levels of single-charged ions created in the resonance Auger process is very important.

EXPERIMENTAL

Measurements of resonance Auger spectra were made at HASYLAB using synchrotron radiation from the storage ring DORIS II in combination with a toroidal grating monochromator. The monochromatic photon beam (band width $\Delta\hbar\omega = 0.45$ eV) was focused onto the interaction zone where it crossed the beam of Rb atoms. The atomic beam was produced by a resistively heated high-temperature oven. Due to high reactivity of Rb it was introduced into the spectrometer in a glass ampoule which was then broken in vacuum applying a special set up. The electron spectra were measured by means of a cylindrical mirror energy analyzer. The energy resolution of the analyzer was 0.8% of the kinetic energy of the electrons. No preradartation was applied during these measurements.

Electron beam excited normal Auger spectra were remeasured at the University of Oulu with the aid of a high-resolution cylindrical mirror energy analyzer. The energy resolution of this analyzer was better than 0.1%. The overall shape of the spectra was much the same as in Ref. 10. The energy calibration of electron spectra was done with the aid of Kr *MNN* Auger spectrum.

RESULTS AND DISCUSSION

Figure 1 displays the energy-level diagram of Rb predicted with the multiconfiguration Dirac Fock (MCDF) calculations applying the computer code of Grant *et al.*¹⁶ The calculated threshold energies for Rb^+ , Rb^{2+} and Rb^{3+} are 3.80, 30.06, and 68.06 eV in a fairly good agreement with the values (4.18, 31.46, and 71.46 eV) given in the literature. This also holds for the $3d$ ionization

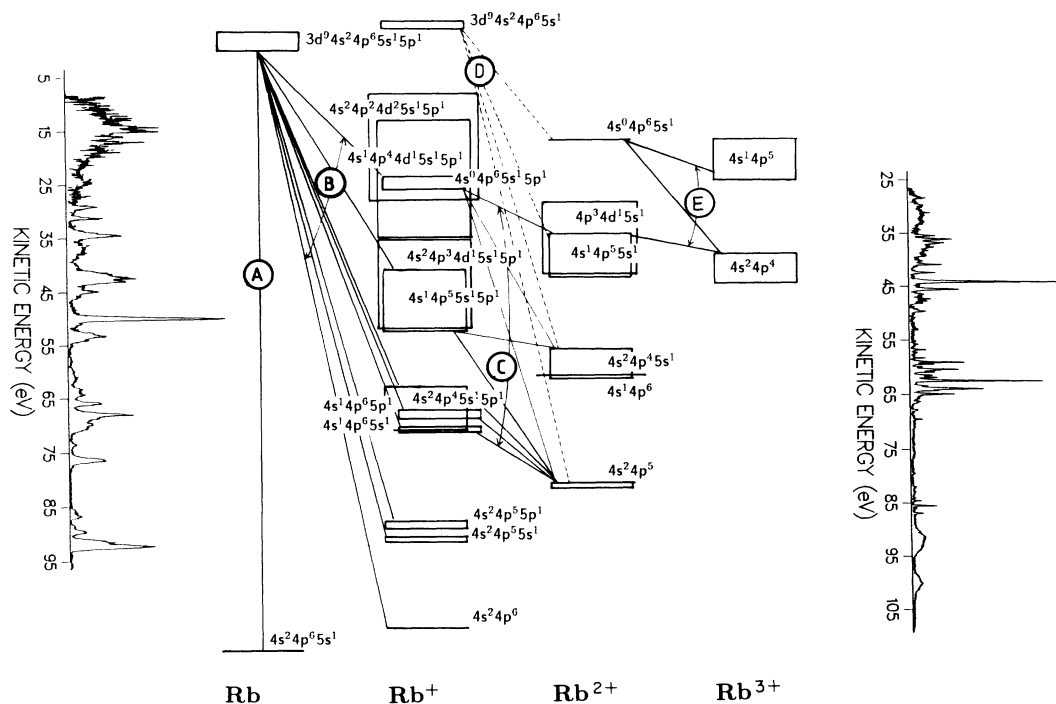


FIG 1. Energy-level diagram of Rb predicted by the MCDF calculations. Left-hand side shows the experimental resonance Auger spectrum (channel *B*) and right-hand side the normal Auger electron spectrum (channel *D*). Both spectra are corrected for the energy-dependent bandpass of the electron analyzer.

thresholds. The calculations place the $3d_{5/2}^5 5s^1$, $J=3,2$ and $3d_{3/2}^3 5s^1$, $J=1,2$ thresholds at 115.9 and 117.4 eV, whereas the experimental values are 117.3 and 118.9 eV.¹⁴ The first maximum in the $3d$ absorption spectrum of RbI was found to be at energy of 113.4 eV by Mansfield and Connerade.¹⁴ Our calculated energies of 112.3–114.1 eV for the energy difference between the ground state $3d^{10} 5s^1$ and the first excited states $3d_{5/2}^5 5s^1 5p^1$; $J=\frac{1}{2}$ and $\frac{3}{2}$ (transition *A* in Fig. 1) agree well with the theoretical predictions of Mansfield and Connerade.¹⁴ The deviation of 1 eV between experiment and theory is probably due to the exclusion of correlation effects (except the s - d mixing) in the calculations.

The photon energy of 113.4 eV used in our experiment is thus able to excite the $3d_{5/2}$ electron to a $5p$ state, where the excited electron most probably stays as a spectator during the Auger-type decay to the levels of Rb^+ . The excited electron can also participate in the process, but according to Koizumi *et al.*¹⁵ this decay is less probable. Their conclusion is based on the absence of any appreciable structure in the Rb^+ ion yield spectra at the energy of the $3d \rightarrow 5p$ resonance. The singly charged Rb^+ ions are almost exclusively produced by direct photoionization of the outer shells. The contributions of participator decays to the Rb^+ states below the lowest Rb^{2+} level (e.g., $3d^9 5s^1 5p^1 \rightarrow 3d^{10} 4s^2 4p^6$, $3d^9 5s^1 5p^1 \rightarrow 3d^{10} 4s^2 4p^6 5s^1$) must be very small.

The experimental electron spectrum is plotted on the left-hand side of Fig. 1. The origin of the kinetic energy scale has been positioned at the $3d^9 4s^2 4p^6 5s^1 5p^1$ reso-

nance. The electron lines originating from decays of the resonance into Rb^+ states (channel *B*) span an experimental energy-level diagram which directly can be compared with the calculated one. Also, the electron lines due to direct photoionization of the Rb $4s$ and $4p$ shells fit into that scheme. The right-hand side of Fig. 1 shows the normal Auger spectrum (channel *D*). The Auger lines mark the energy positions of the Rb^{2+} levels accessible by Auger decay. In order to put our assignment on a firm basis we also have calculated the intensities and profiles of the resonance Auger lines (channel *B*). For comparison the calculated spectrum and the experimental spectrum are presented in Fig. 2.

Next we consider each group of transitions separately. Let us start with the energy region of 60–72 eV first, where the single-configuration predictions are expected to give a good description. The calculated profile of the $3d_{5/2}^5 5s^1 5p^1 \rightarrow 4p^4 5s^1 5p^1$ decay seems to reproduce the experimental spectrum of the energy region in question fairly well as can be seen from Fig. 2. The corresponding normal Auger spectrum ($3d^9 5s^1 \rightarrow 4p^4 5s^1$) (right-hand side of Fig. 1) displays twice the number of structures since the decay of both spin-orbit split Rb^+ $3d^9$ states contributes. The $3d_{5/2}$ component alone displays the same main structures as the resonance Auger spectrum (left-hand side of Fig. 1). Inspection of the peak positions of the experimental spectra shows a clear systematic shift of about 5.3 eV to higher kinetic energies in going from the normal to the spectator Auger spectrum. This shift value compares well with the corresponding value found

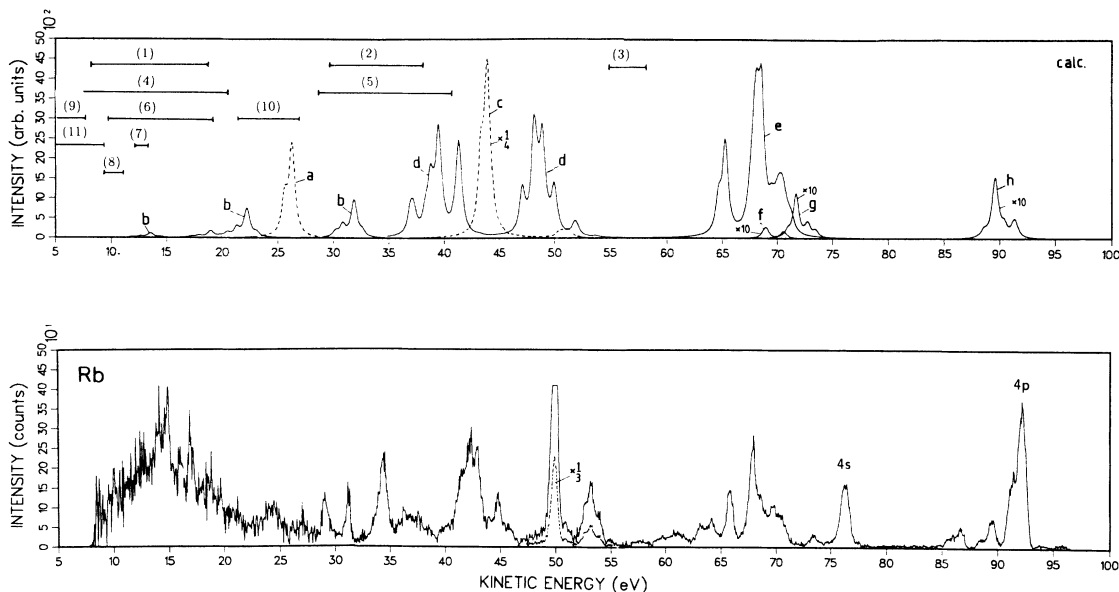


FIG. 2. Experimental (lower part) and calculated (upper part) M_5NV Auger transitions with $5p$ spectator electron for Rb. The characters $a-h$ refer to the transitions in the following way: a , $3d_{5/2}^5 5s^1 5p^1 \rightarrow 4s^0 4p^6 5s^1 5p^1$ (single-configuration prediction); b , $3d_{5/2}^5 5s^1 5p^1 \rightarrow 4s^0 4p^6 5s^1 5p^1 \leftrightarrow 4s^1 4p^4 4d^1 5s^1 5p^1 \leftrightarrow 4s^2 4p^2 4d^2 5s^1 5p^1$ (multiconfiguration prediction); c , $3d_{5/2}^5 5s^1 5p^1 \rightarrow 4s^1 4p^5 5s^1 5p^1$ (single-configuration prediction); d , $3d_{5/2}^5 5s^1 5p^1 \rightarrow 4s^1 4p^5 5s^1 5p^1 \leftrightarrow 4s^2 4p^3 4d^1 5s^1 5p^1$ (multiconfiguration prediction); e , $3d_{5/2}^5 5s^1 5p^1 \rightarrow 4s^2 4p^4 5s^1 5p^1$; f , $3d_{5/2}^5 5s^1 5p^1 \rightarrow 4s^1 4p^6 5p^1$; g , $3d_{5/2}^5 5s^1 5p^1 \rightarrow 4s^1 4p^6 5s^1$; and h , $3d_{5/2}^5 5s^1 5p^1 \rightarrow 4s^2 4p^5 5p^1$. The vertical bars numbered by (1)–(8) show the energy regions of the second- and third-step processes in the following way: (1) $4s^0 4p^6 5s^1 5p^1 \rightarrow 4s^1 4p^5 5s^1$, (2) $4s^0 4p^6 5s^1 5p^1 \rightarrow 4s^2 4p^4 5s^1$, (3) $4s^0 4p^6 5s^1 5p^1 \rightarrow 4s^2 4p^5$, (4) $4s^1 4p^5 5s^1 5p^1 \rightarrow 4s^2 4p^4 5s^1$, (5) $4s^1 4p^5 5s^1 5p^1 \rightarrow 4s^2 4p^5$, (6) $4s^2 4p^4 5s^1 5p^1 \rightarrow 4s^2 4p^5$, (7) $4s^1 4p^6 5p^1 \rightarrow 4s^2 4p^5$, (8) $4s^1 4p^6 5s^1 \rightarrow 4s^2 4p^5$, (9) $4s^0 4p^6 5s^1 \rightarrow 4s^1 4p^5$, (10) $4s^0 4p^6 5s^1 \rightarrow 4s^2 4p^4$, (11) $4s^1 4p^5 5s^1 \rightarrow 4s^2 4p^4$.

recently for Kr. Furthermore, the calculations predict a shift of 5.6 eV for Rb in a fairly good agreement with experiment.

In the case of Kr, a shake up of the spectator electron during the resonance Auger decay was found to result in an extra structure on the low kinetic energy side of the strong lines. The peak structure around 63–64 eV in Fig. 2 is most probably also due to the $3d_{5/2}^5 5s^1 5p^1 \rightarrow 4p^4 5s^1 6p^1$ shake up during the resonance Auger emission. Theory gives a shift of 4.0 eV between shake up and spectator Auger decay which fits well with the observed energy difference. In Rb the shake-up structure seems to be less intense than in Kr, however. Calculated shake-up probabilities, obtained with the overlap integrals between the Rydberg orbital before Auger-like decay and higher Rydberg orbital afterwards, are 0.21 and 0.13 for Kr and Rb, respectively. Figure 3 displays the $5p$ and $6p$ radial wave functions of Rb and Rb^+ . By comparing the $5p$ and $6p$ wave functions of Kr and Rb it seems that the collapse of the $5p$ function during the decay is more pronounced in Kr than in Rb. This may arise from the existence of an extra $5s$ electron in Rb. Thus the shake up seems to be very sensitive also to the outermost electronic structure of the atom.

Inspection of Fig. 1 shows that the energy levels of the $4s^1 4p^5 5s^1 5p^1$ configuration (predicted with the single-configuration approach) do not cover all the experimental structures between 40–55 eV kinetic energy. This is easy

to understand because the $4s^1 4p^5 5s^1 5p^1$ and $4s^2 4p^3 4d^1 5s^1 5p^1$ configurations are degenerate and thus a strong mixing between them is expected. The comparison of the experimental and the calculated spectra in Fig. 2 shows the failure of the single-configuration calculations even more clearly. The single-configuration spectrum (dashed line) displays one very prominent line 6 eV below the line dominating the experimental spectrum. There are almost no counterparts to the experimental

Charge densities of $5p$ and $6p$ electrons

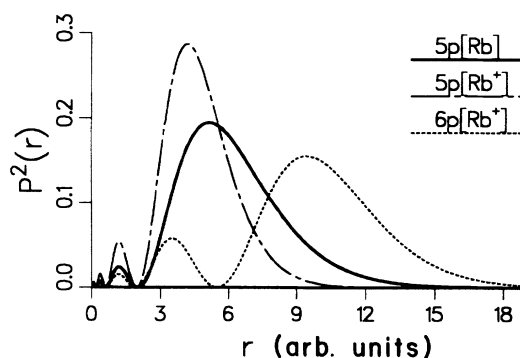


FIG. 3. $5p$ and $6p$ wave functions of Rb.

lines located between 40 and 45 eV and above 50 eV. Taking into account configuration interaction in the final ionic state (solid line) results in a redistribution of the intensity into two groups of lines centered around 39 and 48 eV. The agreement between theory and experiment is better but still far from satisfactory. The absence of the strong line is the most obvious failure of the theory. The energy range spanned by the theoretical and the experimental spectrum is almost the same if we shift the theoretical spectrum towards higher energies by approximately 5 eV. With several open shells the number of levels by far exceeded the number that could be handled in our computations. The discrepancies between the calculated and measured spectrum manifest this shortcoming. The intensity of the correlation satellite structure has been of great interest in many studies of rare gases.^{4,5} By comparing the experimental results for the neighboring elements Kr (Refs. 5 and 7) and Rb it seems that the main line is stronger in Rb, and that the satellites have merged into broad bands. The collapse of the $4d$ function that lies behind the behavior of the satellites is very sensitive to the states of other electrons in the atom. More accurate theoretical calculations with extended basis set are needed, however, for a detailed description of the phenomenon.

The strongest peak in this group [$3d_{5/2}5s^15p^1 \rightarrow 4s^14p^5(^1P)5s^15p^1$] is found to be shifted by 5.75 eV to higher kinetic energy compared to the corresponding line of the normal Auger spectrum (see Fig. 1). The shift is slightly larger than the shift of 5.3 eV observed for the $3d_{5/2}5s^15p^1 \rightarrow 4s^24p^45s^15p^1$ transitions. This indicates small changes in the strength of the electron correlation in passing from the spectrum with spectator electron to the normal Auger spectrum with $4s$ and $4p$ final-state holes.

The degenerate energy levels of the $4s^04p^65s^15p^1$, $4s^14p^4d^15s^15p^1$, and $4s^24p^24d^25s^15p^1$ configurations (see Fig. 1) are also considerably mixed. The redistribution of the intensity at the low kinetic energy side of the spectrum due to this mixing is demonstrated in the upper part of Fig. 2. For comparison the single-configuration prediction is given by the dashed line. In the experimental profile there are additional structures that mainly result from the second step (C in Fig. 1) and third step (E) processes. The kinetic energy regions in which these decays are expected to give rise to structures in the spectrum are depicted in the upper part of Fig. 2. The overlap of many lines explains the broadband observed at low kinetic energies. Some intensity due to second step processes is also expected at higher kinetic energies as indi-

cated by horizontal bars in the upper part of Fig. 2.

Next we turn back to the high kinetic energy side of the spectrum (70–95 eV) where prominent $4s$ and $4p$ photolines accompanied by the satellite and resonance Auger lines are to be seen in the experimental spectrum. The $4s$ and $4p$ hole states can also be reached by the autoionization processes $3d_{5/2}5s^15p^1 \rightarrow 4s^14p^65s^1(g)$ and $3d_{5/2}5s^15p^1 \rightarrow 4s^24p^55s^1$ in which the excited electron participates. On the basis of the ion-yield results their contribution is expected to be small, however, as has been already pointed out. Most of the structure on the low kinetic energy side of the $4s$ photoline (at 73 eV kinetic energy) is due to the $3d_{5/2}5s^15p^1 \rightarrow 4s^14p^65p^1$ decay (f). Its position, as well as the position of the $4s$ photoline, is shifted to higher kinetic energies and some intensity is transferred to the satellites, due to the final ionic state interaction $4s^14p^65p^1 \leftrightarrow 4s^24p^4d^15p^1$. The correlation satellites accompanying the ns ionization also off resonance have been widely studied in the case of rare gases.^{17–20} The interaction seems to be less pronounced in the case of a single $4s$ hole state than in the case of the $4s^04p^65s^15p^1$ and $4s^14p^55s^15p^1$ configurations where a second core hole is accompanying the $4s$ hole. Finally we consider the kinetic energy region of 85–95 eV where the strongest peak is due to the direct $4p$ photoionization. The low kinetic energy side of the $4p$ photoline shows satellites that accompany the $4p$ ionization also at off resonance photon energies, and spectator Auger structure at 89.4 eV due to the $3d_{5/2}5s^15p^1 \rightarrow 4s^24p^55p^1$ transitions (h). The $4p$ satellites are mainly due to $5s \rightarrow 6s$ shake up during the ionization, the calculated energy shift being 5.2 eV and probability 0.14. The $4s$ and $4p$ photolines and their satellites are missing from the theoretical profile (upper part of Fig. 2). Only the spectator Auger transitions predicted by the theory are given, but due to their low intensity, they are scaled by ten.

ACKNOWLEDGMENTS

The authors wish to thank the HASYLAB staff for continuous assistance. The financial support by the Bundesministerium für Forschung und Technologie der Bundesrepublik Deutschland and by the Deutsche Forschungsgemeinschaft is gratefully acknowledged. Two of us (S.A. and A.Y.) are indebted to the Alexander von Humboldt Stiftung for financial support which made their participation in this work possible. Also, the support from the Finnish Academy of Science and Suomen Kulttuurirahasto is gratefully acknowledged.

¹W. Eberhardt, G. Kalkoffen, and C. Kunz, Phys. Rev. Lett. **41**, 156 (1978).

²V. Schmidt, S. Krummacher, F. Wuilleumier, and P. Dhez, Phys. Rev. A **24**, 1803 (1981).

³S. Southworth, U. Becker, C. M. Truansdale, P. H. Kobrin, D. W. Lindle, S. Owaki, and D. A. Shirley, Phys. Rev. A **28**, 261 (1983).

⁴H. Aksela, S. Aksela, G. M. Bancroft, K. H. Tan, and H. Pulk-

kinen, Phys. Rev. A **33**, 3867 (1986).

⁵H. Aksela, S. Aksela, H. Pulkkinen, G. M. Bancroft, and K. H. Tan, Phys. Rev. A **33**, 3876 (1986).

⁶U. Becker, T. Prescher, E. Schmidt, B. Sonntag, and H. E. Wetzel, Phys. Rev. A **33**, 3891 (1986).

⁷D. W. Lindle, P. A. Heimann, T. A. Ferret, M. N. Piancastelli, and D. A. Shirley, Phys. Rev. A **35**, 4605 (1987).

⁸S. Aksela, H. Aksela, H. Pulkkinen, A. Yagishita, M. Meyer,

- Th. Prescher, E. von Raven, M. Richter, and B. Sonntag (unpublished).
- ⁹H. Aksela, S. Aksela, H. Pulkkinen, G. M. Bancroft, and K. H. Tan, *Phys. Rev. A* **37**, 1798 (1988).
- ¹⁰W. Menzel and W. Mehlhorn, *Inner-Shell and X-Ray Physics of Atoms and Solids*, edited by D. J. Fabian, H. Kleinpoppen, and L. M. Watson (Plenum, New York, 1981).
- ¹¹M. W. D. Mansfield and J. P. Connerade, *Proc. R. Soc. London, Ser. A* **344**, 303 (1975).
- ¹²J. P. Connerade with M. W. D. Mansfield, *Proc. R. Soc. London, Ser. A* **348**, 539 (1976).
- ¹³N. Mårtensson and B. Johansson, *J. Phys. B* **14**, L37 (1981).
- ¹⁴M. W. D. Mansfield and J. P. Connerade, *J. Phys. B* **15**, 503 (1982).
- ¹⁵T. Koizumi, T. Hayaishi, Y. Itikawa, T. Nagata, Y. Sato, and A. Yagishita, *J. Phys. B* **20**, 5393 (1987).
- ¹⁶I. P. Grant, B. J. McKenzie, P. H. Norrington, D. F. Mayers, and N. C. Pyper, *Comput. Phys. Commun.* **21**, 207 (1980); **21**, 233 (1980).
- ¹⁷M. Y. Adam, F. Wuilleumier, N. Sandner, W. Schmidt, and G. Wendin, *J. Phys. (Paris)* **39**, 129 (1978).
- ¹⁸K. G. Dyall and F. P. Larkins, *J. Phys. B* **15**, 203 (1982); **15**, 219 (1982).
- ¹⁹H. Smid and J. E. Hansen, *J. Phys. B* **16**, 3339 (1983).
- ²⁰J. E. Hansen and W. Persson, *Phys. Rev. A* **18**, 1459 (1978).